Journal of Hydrology 612 (2022) 128113

Contents lists available at ScienceDirect

Journal of Hydrology

journal homepage: www.elsevier.com/locate/jhydrol

Research papers

Impact of spatial discretization resolution on the hydrological performance of layout optimization of LID practices

Zhaoli Wang [a,b], Shanshan Li [a], Xiaoqing Wu [c], Guangsi Lin [d], Chengguang Lai [a,b,*]

[a] School of Civil Engineering and Transportation, State Key Laboratory of Subtropical Building Science, South China University of Technology, Guangzhou 510641, China
[b] Pazhou Lab, Guangzhou 510335, China
[c] South China Institute of Environment Sciences, Ministry of Environment Protection of PRC, Guangzhou 510535, China
[d] Department of Landscape Architecture, School of Architecture, South China University of Technology, Guangzhou 510641, China

ARTICLE INFO

This manuscript was handled by Corrado Corradini, Editor-in-Chief, with the assistance of Weiping Chen, Associate Editor

Keywords:
Low impact development
Layout optimization
Spatial discretization
Scale effects

ABSTRACT

Climate change and increasing urbanization have worsened urban floods and other water problems, and it is generally accepted that the optimization of the spatial layout of low impact development (LID) practices is a promising solution. Existing studies have focused on coupling the hydrological model with optimization methods, but little is known about the effects of the spatial discretization of the model on the optimization results. In this study, the scale effects were examined in a case study in Guangzhou, China. Four models at various spatial discretization levels, namely models R1, R2, R3, and R4, with an average unit size of $0.022*10^4$, $0.405*10^4$, $2.43*10^4$, and $4.865*10^4$ m^2, respectively, were constructed to investigate the performance difference caused by delineation scales. The results show that the highest-resolution model R1 (one unit represented one type of land cover) provides more cost-effective layout schemes, but during a heavy rainstorm, the solution set provided by a coarser model are very similar to that generated by the finest model R1. A coarser model can provide wider solution sets, but most of these schemes overshadow some types of LID practices such rain garden and bio-retention cell, which also have a critical role in urban heat mitigation, air quality improvement, and so on. Due to the cumbersome work of catchment subdividing and time-consuming optimization process, a coarse model would be a good substitute to a large area. These findings provide new insights on how to achieve better performance by subdividing the catchment at a proper scale when optimizing the spatial layout of LID practices.

1. Introduction

Rapid urbanization not only alters the natural hydrologic cycle, but also changes the surface conditions, for example, replacing vegetation with anthropogenic materials such as concrete, asphalt, brickwork, and metal (Jacobson, 2011). These impermeable materials hinder water infiltration into the soil, increase the formation of runoff and the potential for flooding, and worsen the contamination of water runoff (Bonneau et al., 2017; Li et al., 2020). Meanwhile, it is projected that the impact of global warming will be more severe on urban areas, resulting in more frequent and intense extreme rainfall events (Lai et al., 2020; Javadinejad et al., 2021; Ostad-Ali-Askari et al., 2020; Papalexiou and Montanari, 2019; Yilmaz et al., 2014; Zhang, 2020), which will further complicate urban water management (Marlow et al., 2013).

Traditional centralized measures have the strength of removing more surface runoff rapidly than nature-based solutions, but the construction and renovation work of grey infrastructures are high-priced and it is difficult to offer multiple-benefits, such as pollution load degradation, heat-down, biodiversity and urban amenity (Alves et al., 2019). As such, nature-based strategies have gradually been implemented in many countries, such as Low Impact Development (LID) in the USA, the Sustainable Urban Drainage System (SUDS) in the UK, Water Sensitive Urban Design (WSUD) in Australia, and Sponge City in China (Fletcher et al., 2015). These solutions have appellations but share the same goal, that is, to recover or mimic the natural water cycle in urban areas through nature-based technologies (Chan et al., 2018). One of the most widely used solutions is LID practices, which includes green roofs, rain gardens, vegetative swales, and porous pavements (Dietz, 2007).

Considering their multiple benefits, policymakers prefer LID measures to control surface runoff at its source and mitigate the impacts of urbanization. The variety of LID facilities is considered to be limited (Dietz, 2007), while the number of possible spatial combinations is

* Corresponding author at: School of Civil Engineering and Transportation, South China University of Technology, Guangzhou 510641, China.
E-mail address: laichg@scut.edu.cn (C. Lai).

https://doi.org/10.1016/j.jhydrol.2022.128113
Received 14 December 2021; Received in revised form 18 June 2022; Accepted 21 June 2022
Available online 30 June 2022

deemed to be unlimited. Furthermore, the budget constraints increase the complexity of the selection and placement of LID facilities, as it is expected to achieve higher level of runoff reduction at lower cost. There is an urgent need to seek cost-effective LID layout schemes by balancing conflicting hydrological goal and economic concern (Chui et al., 2016; Kuller et al., 2017; Zhang and Chui, 2018). The exhaustive approach is unlikely to identify the optimal spatial layout for it will take a very long time in most cases to achieve convergence. Instead, with advancements in computational abilities, simulation–optimization approaches emerged and multi-objective optimization algorithms (MOOAs) have been widely used to identify the optimal solution set with several competing objectives (Damodaram and Zechman, 2013; Deb, 2014; Gunantara, 2018; Javadinejad et al., 2019; Ostad-Ali-Askari et al., 2017). Presently, these MOOAs have been successfully coupled with hydrologic/hydraulic models to optimize LID spatial layouts (Islam et al., 2021; Pour et al., 2020). A classic case is the application of the System for Urban Stormwater Treatment and Integration (SUSTAIN) embedded in ArcGIS with general applicability for providing cost-efficient planning schemes under defined constraints (Jia et al., 2015; Lai et al., 2007; Lee et al., 2012; Mao et al., 2017). The essence of this model is the coupling between the Storm Water Management Model (SWMM)/hydrologic simulation program-FORTRAN (HSPF) and the Non-Dominated Sorting Genetic Algorithm (NSGA-II) (Lee et al., 2012). However, one inescapable limitation for utilizing this model is that when it is applied in a large region with complicated pipe networks, its computational burden may be enormous, easily resulting in a program crash. To cope with this deficiency, many researchers have attempted to embed hydrological models into the MOOA framework by coding according to their own research needs. For example, analogous to SUSTAIN, the linking of SWMM and NSGA-II was widely applied (Xu et al., 2017; Oraei Zare et al., 2012; Zhang et al., 2013; Zeng et al., 2020). Furthermore, other algorithms combined with hydrological models have been developed to improve the optimization performance. For example, analogous to SUSTAIN, the linking of SWMM and NSGA-II was widely applied (Xu et al., 2017; Oraei Zare et al., 2012; Zhang et al., 2013; Zeng et al., 2020). Furthermore, other algorithms combined with hydrological models have been developed to improve the optimization performance. For instance, the Long-Term Hydrologic Impact Assessment-Low Impact Development 2.1 (L-THIA-LID 2.1) model was coupled with a multi-algorithm genetically-adaptive multi-objective approach (Liu et al., 2016); the SWMM was linked to the multi-objective antlion optimization algorithm (Mani et al., 2019), the modified particle swarm optimization algorithm (Duan et al., 2016, Li et al., 2019), the multi-objective shuffled frog leaping algorithm (Liu et al., 2019), marginal-cost-based greedy strategy (Xu et al., 2018), or the third Evolution Step of Generalized Differential Evolution (GDE3) (Li et al., 2022).

When it comes to the optimization of LID layout configuration, most researchers have highlighted the effects of different MOOAs on the optimization performance and conducted them at coarse scale, without considering the impact of modelling resolution. It is well known that SWMM is often applied to simulate the hydrological effects of LID facilities (Elliott and Trowsdale, 2007; Qin et al., 2013; Wu et al., 2017; Yazdi et al., 2019). The basic computing units of the runoff component of SWMM are usually the smaller sub-catchments divided from the study area, and the main principle of the subdivision is the spatial variabilities of the landscape such as the distribution of land use types, slopes, and drainage features (Gironás et al., 2010; Rossman and Huber, 2015). Sometimes, there is no uniform standard for the delineation of sub-catchments, and they are mainly determined by modelers so that the scale may be coarse or fine. The uncertainty due to the spatial discretization may affect the surface runoff calculation and the LID layout optimization. Many studies have examined the difference in output from SWMM at various spatial scales, defined here as the resolution of the sub-catchments. In terms of the smaller catchments, it was found that the runoff volumes are relatively insensitive to the spatial resolution (Goldstein et al., 2016; Shaneyfelt et al., 2021; Zeng et al., 2022). For larger watersheds, Sun et al. (2014) observed that the model parameters calibrated based on a fine discretization diminished the uncertainty of the overflow forecasts compared to those of the coarse delineation, and Chang et al. (2019) found that the coarsening of the scale led to a decrease in the total and peak runoff. Similarly, the modeling scale may impact the optimization process of the spatial allocation of LID practices, as the decision variables change with the spatial discretization methods. As LID devices are usually scattered across various sites to mitigate runoff, a fine scale, primarily that a sub-catchment only represents one type of land cover (Rossman, 2010), can reduce the uncertainty of the runoff reduction effects between the actual engineering design and the model output. It is also helpful for the translation of the optimization results into practical measures (Randall et al., 2019), but modeling at finer scales (flat/pitched rooftop, pavements, parking lot, etc.) involves cumbersome work in subdividing, data processing and computation (Chang et al., 2019). Accordingly, the scale issue of the LID layout optimization is a crucial problem in the acquisition of an ideal solution. However, as discussed earlier, previous studies conducted by simulation–optimization approaches mostly employed a coarser model subdivision, that is, lumping diverse land use types into single sub-catchment for simplification, to alleviate the computation burden in the optimization process. Exceptionally, Randall et al. (2019) subdivided the study area into 85,937 sub-catchments by each separate land cover polygons for the convenience of LID allocation, but this study merely examined the hydrological effects under four different LID model scenarios. Bach et al., (2013) quantified the impact of block size on the selection of decentralised stormwater management options using a planning algorithm instead of hydrological simulation. To the best of our knowledge, there is no peer-reviewed literature that investigates the impact of the modeling resolution on the hydrological performance of spatial configurations of LID practices optimized by MOOA.

To bridge the research gap described above, this study aims to explore how the optimal cost-effective curves (i.e., the distribution between investment and runoff reduction rate) change with the scale of the model subdivision under various rainfall conditions. As such, SWMM was selected for modeling at four spatial discretization levels, and then coupled with the GDE3. Finally, we ran them under three design storms with return periods of 0.5, 5, and 20 years. By understanding the modeling scale effects, the findings of this study can provide guidance to modelers and planners hoping to achieve a more cost-effective LID layout, which can reduce more runoff at a lower cost.

2. Materials and methods

2.1. Study area and data source

The Changban Industrial Campus (CIC) in Guangzhou city (23°8′N, 113°16′E), southern China, with a total area of 9.7 ha (Fig. 1), was selected as the study area. The area was affected by the subtropical monsoon, and the annual average precipitation was more than 1720 mm, with heavy rainfall events occurring commonly (Chen et al., 2021). There is a mountain outside the study area, which is located to the north of the study area (Li et al., 2022), and its runoff formation process is rapid and rich during periods of intense rainfall. Furthermore, the CIC is located at a low-lying region with massive impervious surface where large runoff volumes would easily accumulate, and the load of rainwater was prone to exceed the drainage capacity.This highly urbanized area featured commercial buildings with flat or pitched roofs, roads, parking lots, and unexplored territories. As such, this area was prone to flooding due to the synthetic action of substantial rainfall, significant inflow runoff, low-lying terrain, high impervious rate, and low drainage capacity. For example, on 10 May 2016, a heavy rain hit this area, causing severe flooding, destroying the neighboring subway station, several roadway sections, and some low-rise buildings, and causing extensive property damage. Therefore, response options and mitigation measures for reducing the loss caused by flooding is urgently needed in the CIC.

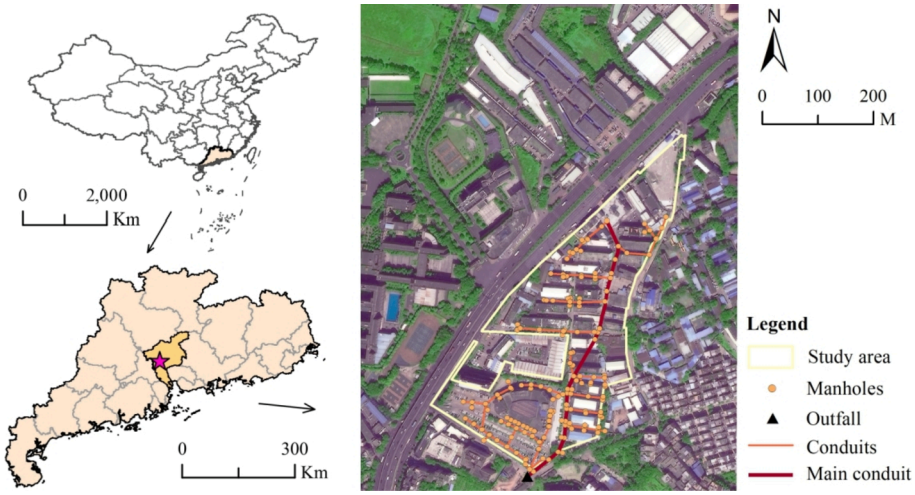

Fig. 1. Location and boundaries of the study area, pipe network and satellite image.

Considering the vulnerability of such areas to flooding, the current land-use type, the existing building layout, and the topography, it is important to adopt the LID layout optimization to such areas to lessen the load of rainwater.

The data required for modeling included the land-use type, as well as a digital elevation model (DEM) with a resolution of 5 m and a drainage network layer lastly updated in 2010, all of which came from the local Land and Resources Bureau and Water Supplies Bureau. An automatic rain gauge and a flow meter were installed at the outfall of the watershed (see Fig. 1) to record rainfall and runoff processes for calibration and validation of the SWMM model.

2.2. Overview and scenarios

In this study, we developed four SWMM models with sub-catchments delineated at four different spatial resolutions, including a high-resolution model (R1) and three progressively coarser low-resolution models (R2, R3, and R4). The storm events with return periods of 0.5, 5, and 20 years were also input into each model as the rainfall series, respectively. Thereafter, inspired by Li et al., (2022) who pointed out that the Third Evolution Step of Generalized Differential Evolution (GDE3) performs better, these models with various rainfall events and discretization scales were embedded to GDE3 (Kukkonen and Lampinen, 2005; Zelinka et al., 2012) to optimize the LID layout. Finally, the data was evolved for 200 and 500 generations, respectively. The straightforward coupling method and the optimization procedure are shown in Fig. 2.

2.3. SWMM model

2.3.1. Model setup at four resolutions

The US EPA Storm Water Management Model (SWMM), composed of runoff and routing modules, has been widely used for dynamic rainfall-runoff simulations in urban areas. There is a LID control module for evaluating the effects of LID practices on runoff reduction (Rosa et al., 2015). As such, we selected the SWMM to carry out the LID layout optimization and eight types of commonly used LID techniques, including the rain barrel, green roof, rooftop disconnection, bio-retention cell, rain garden, porous pavement, infiltration trench, and vegetated swale. One-for-many and one-for-one methods were used to deploy the LID control (Rossman, 2010). The one-for-many method assigns one or more controls to an existing sub-catchment, and the LID practices act in parallel under this option. The one-for-one method occupies the whole sub-catchment by one type of the LID control and it also allows series connection of LID practices in diverse sub-catchments. Shoemaker et al. (2009) has proved that the differences in the simulation results between the distributed and aggregated LIDs were extremely smaller if the area of sub-catchment less than $1.035*10^6$ m^2. As the total area of the study area is only 9.7 ha, the impact of the connection method of LID measures on its efficacy can be neglected. The selection of method mainly depended on the delineation approach of the sub-catchments. When we subdivided the study area at a fine scale with each sub-catchment representing one land-use type, the one-for-one method was suitable for allocating LID practices. Conversely, a sub-catchment delineated at a coarse scale was always comprised of multiple land-use types, which suited the one-for-many method to place the LID facilities. It is worth noting that the decision variables of MOOA,

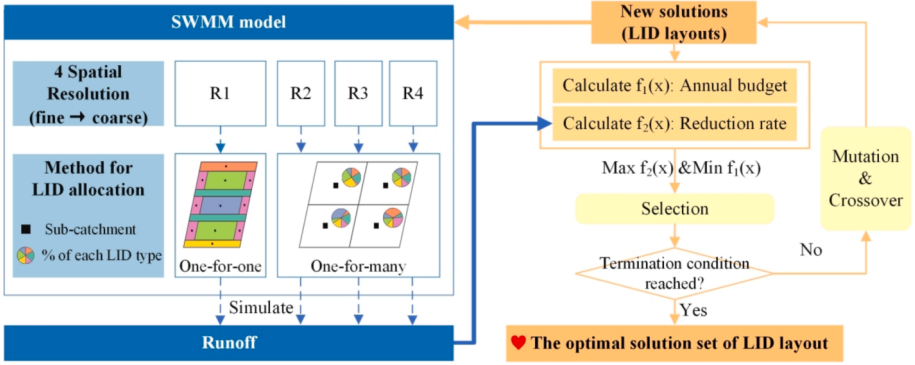

Fig. 2. Flowchart of the coupling between GDE3 and SWMM models with different resolutions (R1, R2, R3 and R4).

which were defined as the number/area of each type of LID facility in each sub-catchment, as well as their constraints varied with partitioning methods, and the distribution of the optimal solution sets changed accordingly. Thus, we developed four versions of SWMM model at different spatial resolution levels, namely, models R1, R2, R3 and R4 (from fine to coarse scale), to investigate the impacts of spatial scale on the allocation optimization of LID practice.

There are two common approaches applied in the urban sub-catchments delineation: geometric method based on nodes and artificial subdivision (Huang and Jin, 2019). The former one automatically generates sub-catchments from the manholes of the urban drainage network by Voronoi (Thiessen polygon). It is time-saving but impractical, for example, a building may be divided into two different sub-catchments. The latter one involves a manual sub-catchment delineation with a comprehensive consideration of the distribution of land cover, elevation, and pipeline network, which is time-consuming but more realistic. As such, we selected the latter method to carry out the subdivision of sub-catchments, and finely divided model R1 into 436 sub-catchments at the microscale according to landscape architects' space requirements and design specifications (Bach et al., 2018). As shown in Fig. 3a, one unit in model R1 always represented a specific land-use type, and the one-for-one method was used to deploy the LID practices spatially. Table S1 (supplementary material) shows the types of LID practices suitable for the specified land cover, and a final list of suitable LID types for each unit would be determined following the field study. Based on the discretization of model R1, these micro sub-catchments were merged into 24 medium sub-catchments to form model R2, which were then combined into four large sub-catchments to shape model R3, and were integrated into two larger sub-catchments to structure model R4 (Fig. 3b). As the sub-catchments in models R2, R3 and R4 always consisted of diverse land-use types, the one-for-many method was the best choice for deploying the LID controls in SWMM. The suitable types of LID practices for each sub-catchment were summarized based on those in model R1. The spatial scales of these four models are different, but they have the same pipe network system that is comprised of 169 junctions, one outfall, and 167 conduits (Fig. 1). The flow direction of each sub-catchment was assigned to a manhole located in the main drainage channel or near the outlet of the sub-catchment.

2.3.2. Design storms

This study also considered the effects of the various rainfall conditions on the layout optimization of the LID practices. As LID practices are always designed to resist a low return period storm event, and the efficiency of LID practices decreased significantly when the return period of the design storm is greater than 20 years (Mei et al., 2018), three rainfall events with 0.5-, 5-, 20-yr return periods were selected to simulate the hydrological performance. According to Intensity-Duration-Frequency (IDF) relationships in Guangzhou, the basic formula of rainfall intensities could be described by formula (1). Based on formula (1), the rainfall intensities of a two-hour duration and the return period of 1 in 0.5, 5, and 20 years were selected to simulate the probable flooding situations, as summarized in Table 1.

$$q = \frac{167A}{(t+b)^n} \tag{1}$$

where q is the rainfall intensity, t is the rainfall duration, and$A$,b, and n are the constants determined by the location of the research region and the return period of the rainfall.

We selected the rainfall pattern with unimodal shapes (middle peak) (Keifer and Chu, 1957; Marsalek and Watt, 1984), which is widely applied in current engineering practices, to distribute the rainfall intensity temporally (Liu et al., 2015). The time-to-peak ratio could be expressed as$r = t_p/t_d$, where t_p is the time before the peak value, and t_d is the duration of total rainfall. The value r is an essential parameter in design storms, and it is empirically fixed at 0.48 in Guangzhou according to historical storms. The temporal resolution is 1 min, and the equations of the design storm could be expressed as formula (2):

Table 1
The formula of rainfall intensities under various return periods.

Return period	Formula 167*A / (t + b)^n
0.5	167*39.29 / (t + 16.812)$^{0.911}$
5	167*32.406 / (t + 12.874)$^{0.758}$
20	167*24.917 / (t + 8.406)$^{0.653}$

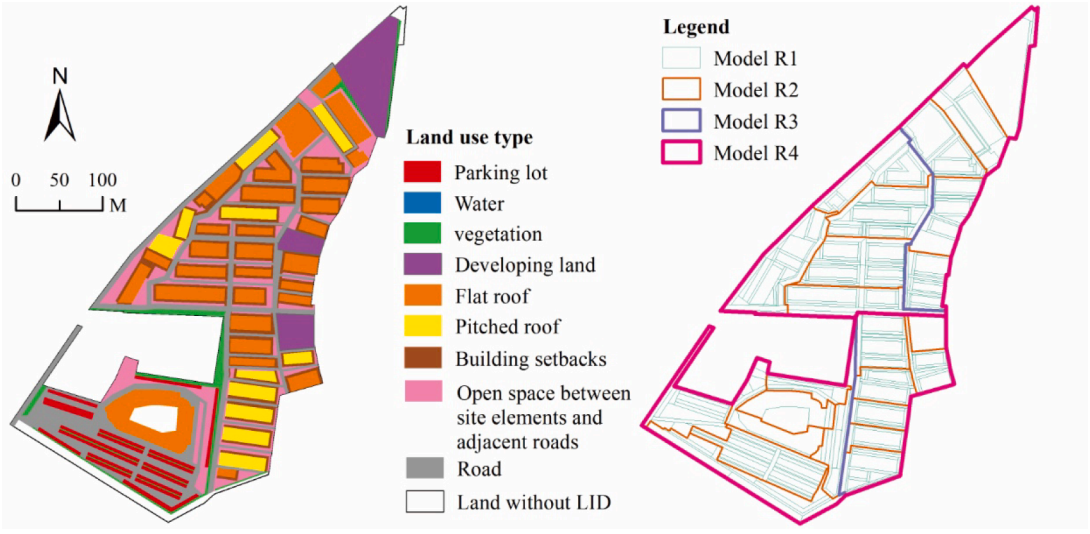

Fig. 3. (a) The distribution of land type, and (b) different catchment delineation of the study area (Sub-catchments with green borders constitute model R1, sub-catchments with orange borders constitute model R2, sub-catchments with grey violet borders constitute model R3, and sub-catchments with royal pink borders constitute model R4.). (For interpretation of the references to colour in this figure legend, the reader is referred to the web version of this article.)

$$i_t = \frac{A}{(\frac{\tau}{\rho}+b)^n}(1-\frac{n\tau}{\tau+\rho b}) \quad (2)$$

where $\tau = t_p - t$ and $\rho = r$ for $t \leqslant t_P$,

$\tau = t - t_P$ and $\rho = 1 - r$ for $t > t_P$,

i_t is the rainfall intensity at time t, and the constants A, b, and n correspond to the constants A, b, and n in formula (1), which differ with the various return periods (Table 1).

2.3.3. Calibration and validation

There are two types of parameters, namely, measured and empirical parameters, in the SWMM model. The measured parameters are the area, width, slope, and impervious percentage of each unit, and they are determined by the topography and land cover type. In this case, the area and slope were calculated automatically in ArcGIS, the width of the sub-catchment was calculated by taking the square root of the sub-catchment area, assuming each sub-catchment to be square in shape (Bisht et al., 2016), and the impervious percentage was computed based on the distribution of land use. As the sub-catchments in model R1 had the highest resolution, the impervious percentage of model R1 could be determined quickly and accurately, and the impervious percentages of models R2, R3 and R4 were calculated based on that of model R1. The invert elevation and the maximum depth of each junction were other measured parameters that were extracted from the municipal pipe network database. As for the empirical parameters, the Manning value of the surface, the storage depth, and the Horton-based infiltration indicators were initially established by referring to the adjacent catchment area (Chen et al., 2018; Zeng et al., 2019) and the SWMM manual (Rossman and Huber, 2015). The recommended ranges and values of calibrated parameters for SWMM are shown in Table S2. The infiltration rate is very important in model calibration as the soil in Guangzhou is relatively moist during the rainy season (from June to October). Consequently, the Manning value, the depth of depression storage on impervious/pervious area and maximum/minimum infiltration rate within the recommended ranges of parameters were adjusted to improve the model accuracy. Generally, one parameter was modified at a time when other parameters were fixed, and we repeated this process until the requirements of NSE values were met. As the model was well calibrated after these steps, it was not necessary to adjust the characteristics width.

The observed rainfall event from 2:10 of Jun 7 to 19:55 of Jun 8 in 2018 was used to calibrated model R3, and then another measured event, from 12:25 of Aug 28 to 5:35 of Aug 29 in 2018, was applied to validate. The Nash-Sutcliffe Efficiency (NSE) value was greater than 0.7 for both calibration and validation periods, and it is generally acceptable of NSE greater than 0.5 (Moriasi et al., 2007; Nash and Sutcliffe, 1970). The shape and timing of the simulated hydrograph showed good agreement with the observed data, with very slight differences at the peaks, as shown in Fig. 4. Next, the validated parameter values of the low-resolution model R3 were used to calibrate and validate the model R1, R2 and R4. It was found that the simulated hydrographs of models R1, R2 and R4 almost coincided with that of model R3 (Fig. 4), and all NSE values were greater than 0.7 (Table 2). This indicates that the level of sub-catchment discretization has little impact on the overall model performance, which is supported by previous studies on the scale effects (Shaneyfelt et al., 2021;Goldstein et al., 2016; Ghosh and Hellweger, 2012). As such, models with various spatial resolutions perform well in the hydrological simulation, and they can be considered for further study in scale effects.

The calibration parameter values were set as follows: the Manning's value and depression storage's depth of the impervious area were 0.011 and 0.5 mm, and those of the pervious parts were 0.24 and 1 mm, respectively; the maximum and minimum infiltration rates were 10 mm/h and 1.25 mm/h, respectively, and the decay constant value was 4; and Manning's value of the channel was between 0.01 and 0.01.

2.4. Multi-objective optimization algorithm – GDE3

2.4.1. Definition of optimization problem

In this study, we adopted the GDE3 to investigate the scale effect on the distribution of the optimal solution sets of the LID layout. The multi-objective optimization problem (Deb, 2014) considered here consisted of finding a set of decision variables $\mathbf{x} = (x_1, x_2, \ldots, x_n)$, corresponding to the number/area of each LID practice type in each sub-catchment, which minimized the total annual budget $f_1(x)$ and maximized the runoff reduction rate $f_2(x)$, expressed as formula (3). Improvements in hydrological performance always result in increased investment, so the optimal solution does not exist and the MOOA is always employed to balance these conflicting goals to get a set of optimal solutions.

$$min f_1(x) = \sum_{j=1}^{m}(A_{1j} + A_{2j}) \text{and} \max f_2(x) = \frac{Runoff_{baseline} - Runoff_{LID}}{Runoff_{baseline}}$$

Table 2
Nash-Sutcliffe efficiency (NSE) metrics for different models.

		Model R1	Model R2	Model R3	Model R4
Calibration	Jun 7, 2018	0.725	0.735	0.73	0.737
Validation	Aug 28, 2018	0.767	0.763	0.763	0.789

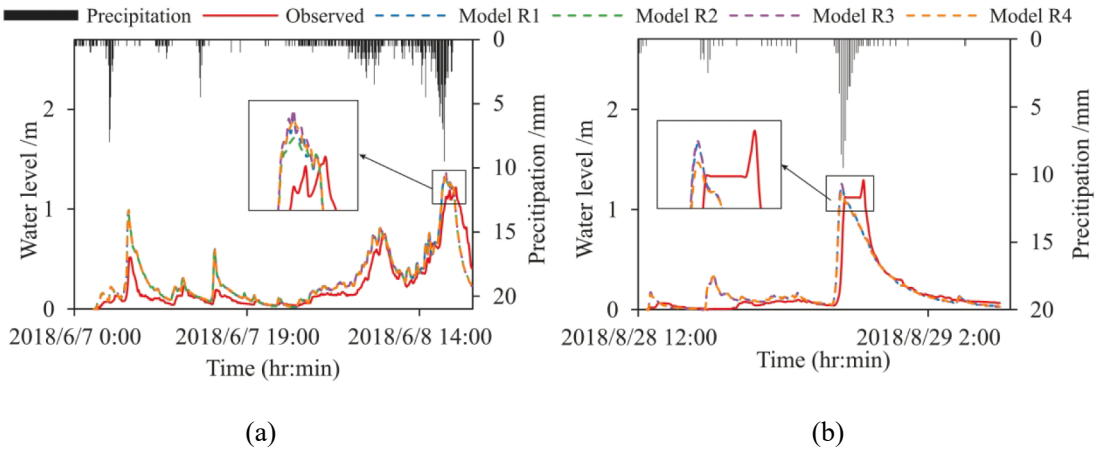

Fig. 4. Hydrographs comparing of models with different resolutions. (a) Rainfall event from 2:10 of Jun 7 to 19:55 of Jun 8 in 2018 for calibration; (b) rainfall event from 12:25 of Aug 28 to 5:35 of Aug 29 in 2018 for validation.

where A_{1j} and A_{2j} are the annualized construction cost and the annual maintenance cost (Huang et al., 2018) of the LID practice$j$, respectively; m is the number of varieties of the LID facilities that can be used at a sub-catchment; $Runoff_{baseline}$ and $Runoff_{LID}$ are the simulated runoff in the scenario without and with the LID layout, respectively. Once the construction of the LID practice was completed, yearly maintenance was required over its entire life for the regular operation of the LID facility. As the lifetime varied with the type of LID practice (Table 3), we adopted the total annual budget as an economic performance indicator. The initial construction cost P_j was uniformly transformed into the annualized construction cost A_{1j} over a n_j-year project lifetime at an annual real interest rate of$i$, which could be expressed as equation (4):

$$A_{1j} = P_j \frac{i(1+i)^{n_j}}{(1+i)^{n_j}-1} \tag{4}$$

The one-for-one method to place LID practices (Rossman, 2010) was always applied in models with fine-resolution sub-catchments, and landscape architects and urban planners were invited to identify the suitable LID sites and subdivide the study area into small units based on the site feasibility (Table S1), landscape architecture, and local construction guidelines (Bach et al., 2018). There were several alternative types of LID implementation on a site, but only one could be selected at one run. Accordingly, the decision variables $\mathbf{x} = (x_1, x_2, ..., x_n)$ referred to the selected type of the LID practice in each unit. The type of LID practice selected for the n^{th} sub-catchment isx_n, and it was chosen from a list of types of LID practices that were suitable for the n^{th} sub-catchment. Correspondingly, the range of x_n was one of the values in$\{0,1,...,t\}$, where 0 represents no LID facility was built in the n^{th} sub-catchment, t is the sum of the types of LID practices that can be placed in sub-catchment n, and the codes from 1 to t represents different types of LID practices. Such as, in terms of the sub-catchment made up of a flat roof,$x_n \in \{0,1,2\}$, in which 1 represented green roof and 2 represented rain barrel. This means that the lower bounds of all decision variables were set to 0, while the upper bounds depended on the number of the types of LID practices that were feasible to build in the corresponding sub-catchment.

However, the one-for-many method was more suitable for the model with coarse-resolution sub-catchments. There were several varieties of land cover in a sub-catchment, so it could simultaneously contain multiple types of LID facilities. As such, the decision variable was altered to the area of each type of LID practice at each sub-catchment, expressed as $\mathbf{x} = (x_{11}, x_{12}, ..., x_{1k}, ..., x_{m1}, x_{m2}, ..., x_{mk})$, where k is the type of LID practice, m is the sub-catchment number. There are two constraints: one is that the value of x_{mk} must not be greater than the suitable area in the m^{th} sub-catchment for the LID practice$k$, and the other is that the sum of the area of each type of the LID practice allocated at the m^{th} sub-catchment ($x_{m1}, x_{m2}, ..., x_{mk}$) must be less than or equal to the total area of sub-catchment$m$.

Table 3
Life cycle and cost of each adopted LID practice.

	Life cycle (year)	Annualized construction cost	Annual maintenance cost	Total cost
Green roof	60	6.9	9.2	16
Rain barrel	5	125.2	0.8	126
Rooftop disconnection	5	0.8	0.8	2
Porous pavement	15	9.8	2.3	12
Rain garden	80	8.5	12.3	21
Bio-retention cell	80	16.1	12.3	28
Vegetated swale	8	2.5	1.2	4
Infiltration trench	7	5.6	1.1	7

Note: the cost unit of the rain barrel is USD/per rain barrel, and the cost unit of other LID practices is USD/m^2.

2.4.2. Development of GDE3

Numerous studies have demonstrated that there is no single algorithm outperforming the others (Huo et al., 2016; Keshavarzzadeh and Ahmadi, 2019; Quresh et al., 2019; Vargas et al., 2021) and the preferred algorithm depends on the definition of the optimization problem such as the number of decision variables and constraints. Since the goal of this study is to examine the scale effect, based on the study conducted by Li et al., (2022), the Third Evolution Step of Generalized Differential Evolution (GDE3) was chosen to optimize the placement of LID practices due to its prominent mutation and crossover operators. The overall structure can be expressed as follows:

1. Initialize the parent population of the size NP randomly with values from the specific range. As the decision variables in model R1 changed within a small number of discrete values and there was no constraint, the initial values of parent population was generated randomly. For models R2, R3, and R4, the ranges of decision variables consists of a large number of discrete values. More importantly, there were many solutions that did not satisfy the defined constraints. As such, values that located at one-quarter or one-fifth of the ranges while meeting the restrictions were used as initial solution to ensure the smooth progress of the optimization.
2. Repeat until the termination condition is satisfied:
   a) Generate offspring population after repeating NP times:
      i. Select a point from the parent population
      ii. Generate a new offspring point with mutation and crossover
      iii. Update the impervious rate and width for a new offspring point (Rossman, 2010)
   b) Combine the parent and offspring populations.
   c) Select the best NP points for the subsequent evolution according to fast non-dominated and crowding distance sorting.

The outstanding characteristic of the GDE3 is its mutation and crossover operators, which act on each element of each solution through internal loops. The GDE3 is an extension of the differential evolution (DE) algorithm, whose crossover and mutation operations are determined by the crossover rate ($CR \in [0,1]$) and the mutation factor ($F \in \mathbb{R}$). P_G is a population of NP solution vectors (sets of decision variables) $x_{i,G}$ in a generation$G$, and $i \in \{1, 2, 3, ..., NP\}$ is a vector index. Each $x_{i,G}$ is an n-dimensional vector, and $x_{j,i,G}$ is its j^{th} element ($i \in \{1,2,3,...,n\}$). Three solution vectors, namely,$x_{p_1,G}$,$x_{p_2,G}$, and $x_{p_3,G}$ that are mutually different and different from $x_{i,G}$ are randomly selected from the parent population.$x_{j,p_1,G}$,$x_{j,p_2,G}$, and $x_{j,p_3,G}$ were the j^{th} elements of$x_{p_1,G}$,$x_{p_2,G}$, and$x_{p_3,G}$, respectively. A trial element $y_{j,i,G}$ is generated by crossover operations and a trial vector $y_{i,G}$ is obtained after the loop (See Fig. S1 in the supplementary material).

3. Results

3.1. Performance differences between generations

In this study, a population size of 200 was evolved for generations 200 and 500 to examine how generation affected optimization results of models at various resolutions. As the solution sets were discrete, the solutions under various scenarios did not always have the same cost or reduction rate. For the convenience of data analysis, when calculating the difference in the reduction rate between the different scenarios, the two points with the closest cost were selected for comparison. The average percent differences in the reduction rate (with respect to 200 generations) for 500 generations (AvPD-Ge values) are listed in Table 4. For model R4 with the lowest resolution, the AvPD-Ge values are relatively minor (less than0.38%), indicating that the front curve remains

Table 4
Average percent difference in reduction rates between 200 generations and 500 generations (AvPD-Ge).

	Model R1	Model R2	Model R3	Model R4
P = 0.5a	3.77	2.78	1.75	0.38
P = 5a	5.79	2.88	0.35	0.33
P = 20a	3.18	1.62	0.33	0.24

stable when the generation reached 200, and further evolution is unnecessary. The AvPD-Ge values rise with the increase in resolution. The AvPD-Ge values for higher-resolution models R1 and R2 range from 1.62 % to 5.79%, which indicates that models at finer scale are more sensitive to generations. The number of decision variables for models R1, R2, R3 and R4 are 430, 192, 32 and 16, respectively. As a result, this may be explained by the fact that models at finer scales have more decision variables, requiring more generations to yield a stable optimal solution set. Additionally, it is worthwhile to note that, as shown in Table 5, it takes significantly longer to optimize higher-resolution models; however, while model R1 has twice as many decision variables as model R2, the difference in processing time is relatively small. This is because, for model R2, the range of decision variables is much boarder, and there is a requirement to select solutions that satisfy the constraints during the optimization process.

3.2. Scale effects on the LID layout optimization

Following the results in Section 3.1, it is hypothesized that the solution sets reach a more stable state after 500 generations. These results were then used to analyze the effects of modeling scales on the LID layout optimization under the rainfall events of the return periods of 0.5, 5, and 20 years, as shown in Fig. 5. It is evident that the distribution ranges of solutions produced by models R1 and R2 are the narrowest regardless of the type of rainfall event, but most runoff reduction rates computed by model R1 are higher than those computed by other models, particularly for the 0.5-yr and 5-yr rainfall events. It is suggested that for the low-intensity rainfall events, the layout schemes of LID practices optimized by model R1, in which one-for-one methods are applied to deploy LID practices spatially, could reduce runoff more effectively at the same cost point. In addition, the front curve for model 4 has the greatest coverage and most cost-effective schemes, followed by model 3 and finally model R2. This result indicates that when applying the one-for-more method to place LID practices, the coarser the sub-catchment resolution is, the better the performance of optimizing LID layouts would be. It might also be related to the variation in the number of decision variables, since the number of decision variables decrease as the spatial scale become coarser. More importantly, as the return period of rainfall events increase, the differences between the front curves of Models R1, R2, R3 and R4 become smaller and tend to merge together. That is, the modelling scale has less impact on optimization layout of LID practices under high-intensity rainfall events.

Based on each solution on the front curve (see Fig. 5), the total area occupied by each type of LID practice was calculated and plotted against the resolution of the sub-catchment discretization, as shown in Fig. 6. Outliers are solutions that were numerically out of the ordinary. Apart from outliers, the area of LID practice generally varies within the interquartile range. For instance, under the 0.5-yr rainfall event, the total area of green roofs ranges from 0 to $1.3*10^4$ m^2 when optimizing model R1. This spread, however, changes to 0 to $0.4*10^4$ m^2, 0 to $2.2*10^4$ m^2, 0 to $2.3*10^4$ m^2 when optimizing model R2, R3 and R4. It can be seen that the variation range of areas occupied by each type of LID facility for model R1 is smaller in comparison with other models. This is in agreement with the fact that the spread of optimal solution sets of model R1 is also smaller. Besides, for model R1, there is few rain barrel and rooftop disconnection applied in the layout design; and with the increase of return period of rainfall event, the variation range of rain garden and bio-retention cell is low, whereas the distributions of area of green roof, vegetated swale, infiltration trench, and porous pavement change dramatically. In the Model R2, the area covered by rainfall barrels, rooftop disconnection, rain gardens, and bio-retention cells is little, and most of the space is reserved for infiltration trenches and porous pavement. For models R3 and R4, the variation ranges of green roof, vegetated swale, infiltration trenches and porous pavement is broad, and more rooftop disconnections and rain garden were used in the layout design. The results indicate that models with varying resolutions prefer different type of LID practices to optimize their layout schemes.

Table 5
Comparison of elapsed times for each model when it optimized for generations 200 and 500 (unit: hour).

	Model R1		Model R2		Model R3		Model R4	
	200	500	200	500	200	500	200	500
P = 0.5a	1.23	3.16	1.87	3.85	0.56	1.27	0.46	1.02
P = 5a	2.21	5.29	1.9	4.05	0.58	1.32	0.46	1.12
P = 20a	2.15	5.1	1.82	3.9	0.49	1.33	0.46	1.13

3.3. LID layout at a specific target

As can be seen in Fig. 5, the maximum runoff reduction rate for model R1 is about 60%. For the purpose of ensuring a clear understanding of LID layout schemes, a 60% runoff reduction was selected to analyze the difference of the spatial distribution of LID facilities for models R1, R2, R3 and R4, as illustrated in Fig. 7. In each sub-catchment, a pie chart was created to illustrate the relative proportion of each type of LID practice. From the layout map of model R1, it is clear what type of LID practice should be located where. In comparison with other models, the layout generated by Model R1 can serve as a design scheme for implementation in a practical setting. Nevertheless, from the layout of model R2, R3, and R4, we can only estimate the proportions of each type of LID practice to be deployed within each sub-catchment.

Additionally, layouts for a 20-yr rainfall event were applied to two real rainfall events described in Section 2.3.3 and and a 50-yr design rainfall event in order to analyze differences in hydrological responses between optimized models at various discretization scale. Table 6 shows that the differences in the reduction rate between the schemes of each model are very small (less than 1.46%) during a 50-yr rainstorm, while the difference during two real rainstorms varies within 6.33%. The scheme optimized by model R4 performs the worst regardless of the type of rainfall; besides, the layouts generated by models R1 and R2 are able to capture more runoff during the rainfall events of Jun 7 and Aug 28, respectively. It can be found that the reduction rates of model R2 are relative high under these two ocnditions, but its budget is also the highest at $61.25*10^4$ USD. In other words, the optimal layout of model R2 achieves a similar runoff control target (60%) at a higher cost than other models under a 20-yr rainstorm, but it can capture more runoff under the rainfall events with different shapes. This indicates that the hydrological performance of LID layout are sensitive to the patterns of rainfall events.

4. Discussion

4.1. Implication and cause analysis

As mentioned previously, most studies have focused on embedding the SWMM model into various MOOAs to improve the performance of the layout optimization of LID facilities, while ignoring the scale effects caused by the spatial delineation of the SWMM model. By contrast, the present study reveals the impact of sub-catchment resolutions on the layout optimization of the LID facilities during rainfall events with varying intensities, which could facilitate the selection of an appropriate spatial discretization scale to optimize the layout of LID facilities.

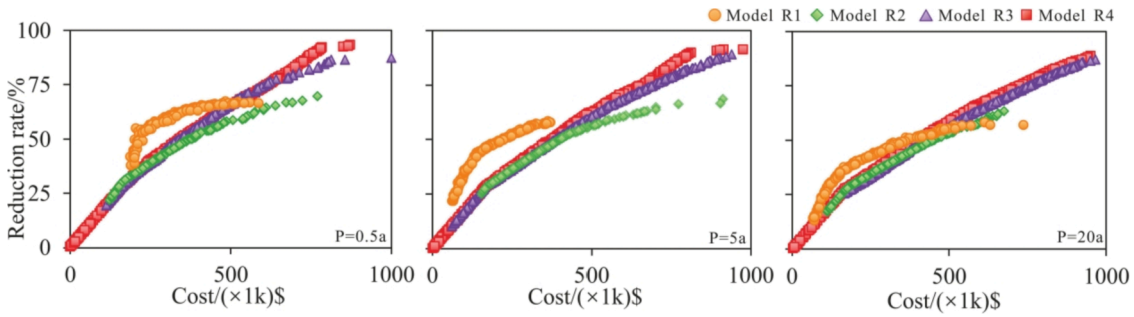

Fig. 5. The scale effects on cost-benefit curves under various rainfall events with return periods of 0.5, 5 and 20 years. The y- and x-axis represent the reduction rate of the outfall outflow volume and the total annual budget, respectively.

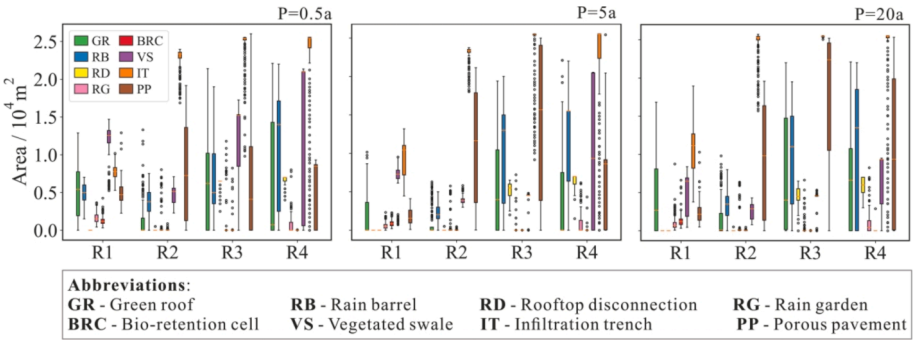

Fig. 6. Statistical comparison of areas occupied by various LID designs at R1, R2, R3 and R4 model resolutions.

The results show that, for a given cost, runoff control effectiveness of the layout optimized by each model decreases with the increase of return periods of rainfall event, which is in line with previous studies that the performance of LID practices decreases with the growth of rainfall intensity (Lee et al., 2013; Qin et al., 2013; Yin et al., 2020). This indicates that the main purpose of LID facilities is to resist small storm events. It is worth noting that this decline is more pronounced in model R1. In the beginning, it was suspected that this was related to the inadequacy of the evolution generations, and we then used the GDE3 to optimize model R1 under a 20-yr rainstorm for 1000 generations. However, the increase in generations only slightly enhances the performance of the layout optimization, so the effect of generation on the distribution of optimal solution sets can be disregarded. It was also observed that the coarser the spatial resolution, the broader the spread of optimal cost-effective solutions; the finest model R1 could provide better LID layout schemes at a lower cost, especially for low-intensity rainfall events, but for the models R2, R3, and R4, the cost-effectiveness of solutions decreases with increasing spatial resolution. This can be explained by the different number of decision variables and their ranges present in each model, since the data (i.e. elevation, land use, and drainage network) used for SWMM modelling were the same. A finer model always has a higher number of decision variables, like 436 in model R1, 192 in model R2, 32 in model R3, and 16 in model R4. However, despite having a greater number of decision variables, the ranges of decision variables in model R1 are the narrowest, only consisting of a list of types of LID practices. When applying one-for-more method to place LID facilities, the ranges of decision variables increase with the decline of the number of decision variables. Differences caused by spatial resolutions, such as the number of decision variables and their ranges, collectively affect optimization performance. Another significant advantage of model R1 is that its solution set can take into account high-cost LID practices such as rain gardens and bio-retention cells to achieve the flood control. Yet models R2, R3 and R4 prefer low-cost alternatives such as porous pavement, vegetated swales, and infiltration trenches. As such, in spite of similar performance on runoff control, solutions provided by R1 have addition benefit in conserving biodiversity, mitigating urban heat and improving air quality. However, constructing model R1 with units representing one type of land cover requires researchers to conduct a field study to determine which type of LID practice can be deployed and subdivide the catchment carefully, and it is also time-consuming to optimize model R1. As such, it is not recommended to apply the subdividing method like model R1 to a large area.

It can be found that when applying one-for-more method to distribute LID facilities, coarser model can provide more cost-effective layout schemes. But it does not mean that a coarser model always performs better, as the results showe that model with a coarser resolution may perform poorly under other rainfall patterns. This suggests that further testing is required to understand the trade-offs between spatial scale, rainfall pattern and the optimal solution sets. Another important finding is that during the high intensity rainfall event (P = 20a), the distributions of optimal sets for models at various scales are very similar. Perhaps this is due to the fact that a coarser model has the ability to increase the proportion of LID practices with lower costs, such as porous pavement, infiltration trench, and vegetative swales. Then when the study area is large, it is recommended to delineate sub-catchments at a moderate scale for optimization in order to save time in processing data whilst achieving better front curves.

4.2. Advantage and deficiency of the study

As opposed to previous studies (Li et al., 2022; Liu et al., 2019), which aimed to improve the performance of LID layout by applying different MOOAs, the objective of this study is to examine the scale effects on the optimization of LID deployment. One of the most significant findings is that when the one-for-more method is adopted to place the LID practices, the study area could be coarsely delineated to reduce runtime without comprising performance. Another finding is that the fine model, deploying LID practices by the one-for-one method, could provide more cost-effective solutions with multi-type LID practices, but

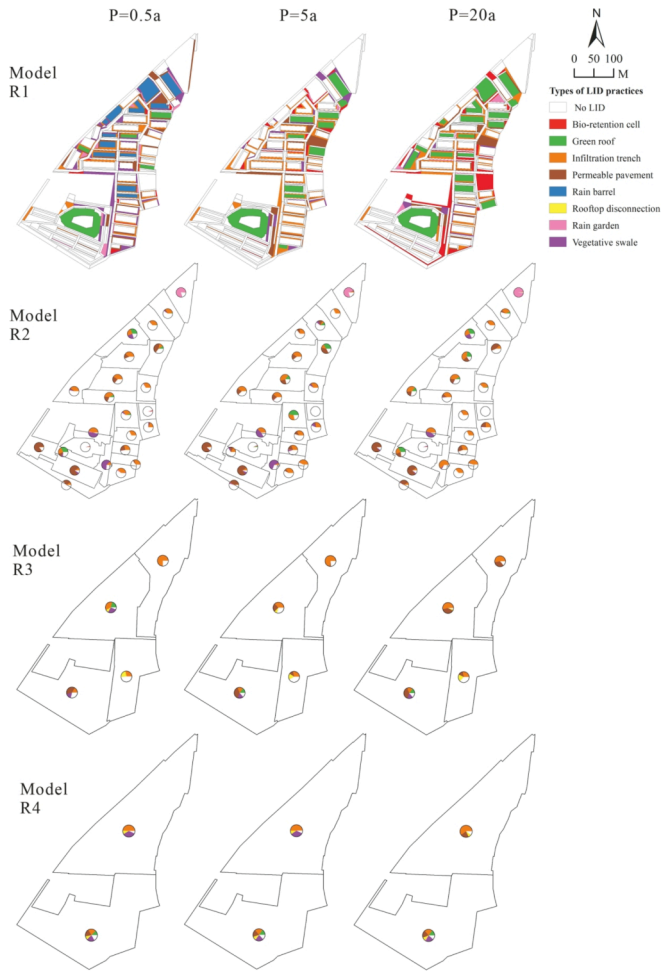

Fig. 7. Spatial layouts of various LID facilities at a 60% runoff reduction.

Table 6
Reduction rate of the optimized model applied to the measured rainfall event.

	Model R1	Model R2	Model R3	Model R4
Cost ($\times 10^4$USD)	61.35	62.39	54.42	51.39
P = 50a	55.43%	56.54%	56.64%	56.89%
Jun 7, 2018	51.47%	50.39%	46.99%	45.14%
Aug 28, 2018	60.36%	63.32%	64.31%	59.04%

the preliminary subdividing work and optimization process is much more cumbersome and the spread of optimal cost-effective solutions is narrow. The results can guide modelers in selecting appropriate spatial delineation methods, which has not yet been explored in previous studies. In the case of a small urban area, a fine model with one-for-one method would be preferred, as its layout could offer multiple functions and could be directly applied in practice, thus reducing budget waste resulting from the gap between research and application. To a large area, it is recommended to obtain an initial optimization result at a coarse scale as a guideline for urban planning, and then refine a fine-scale layout design for a specific area when applied to engineering practice. Therefore, it is worth taking the time to conduct this research.

However, some deficiencies remained in this study. For example, due to limited data availability, only one study area (9.7 ha) was applied to examine the scale effects of the layout optimization, so it is more suitable to apply the conclusion into a urban catchment with similar size. More general conclusions should be drawn by taking larger or smaller areas as examples. Based on the previous study conducted by Li et al., (2022), only one MOOA, the GDE3, was selected to analyze the optimization performance of the LID deployment. The results were privately compared to those optimized by the commonly used NSGA-II, and the comparison shows that the performance differences between these two MOOAs could be ignored. Optimal results might be improved if an algorithm is tailored specifically to the layout problem of this study, such as a finer-scale model with a narrow solution set, was proposed. As discussed in section 4.1, the layout optimization of LID practices may also be influenced by patterns of rainfall events, such as bimodal, uniform, and unimodal (with early peak and late peak) shapes (Zhang et al., 2021). It is also a challenging undertaking to determine which rainfall event should be used to optimize the model. Furthermore, LID practices serve multiple functions in urban design, such as cooling, amenity, sanitation, and biodiversity, and these factors should be taken into account for the layout optimization of LID practices in the future study.

5. Conclusion

In this research, we took the CIC in Guangzhou, China, as the case study to investigate the effects of the modeling scales on the LID layout optimization. The SWMM model was used to simulate the hydrological response of each layout, which involved two types of LID deployment approaches, namely one-for-one and one-for-many. When applying one-for-one method, the model R1 with the finest resolution can provide more cost-effective layout schemes consisting multiple types of LID practices, but this advantage is diminished during a 20-yr rainstorm. The solution set of the finest model R1 is the narrowest, and it can not provide layout schemes with higher runoff reduction rate (>60%). Additionally, considerable time and effort must be invested in the sub-catchment delineation and optimization process for the finest model R1, which did not suit a large area. However, the coarser models (R2, R3, and R4), which applied one-for-more method to place LID practices, can achieve a wider solution set while yielding similar benefits during a heavy rainfall event. Therefore, if a high-intensity rainfall event is selected to carry out SWMM model, it is more appropriate to apply a coarser model at the planning stage to ensure the investment and runoff control targets, whereas the finest model is better suited to be applied at the implementation stage to provide a layout that covers a variety of LID practices and their corresponding sites.

In summary, our findings provide new perspectives on the selection of spatial discretion resolutions in the LID layout optimization process. However, rainfall pattern and regional differences should also be noted when examined the scale effect of LID layout optimization. For future studies, it is suggested that various rainstorm patterns and case studies should be considered so as to minimize uncertainties as much as possible and achieve more reliable results.

CRediT authorship contribution statement

Zhaoli Wang: Conceptualization, Project administration, Funding acquisition, Resources, Writing – original draft. **Shanshan Li:** Methodology, Validation, Formal analysis, Writing – original draft. **Xiaoqing Wu:** . **Guangsi Lin:** Writing – review & editing. **Chengguang Lai:** Conceptualization, Resources, Writing – review & editing, Supervision, Funding acquisition.

Declaration of Competing Interest

The authors declare that they have no known competing financial interests or personal relationships that could have appeared to influence the work reported in this paper.

Data availability

Data will be made available on request.

Acknowledgements

The research acquire financial or data support by the National Key R&D Program of China (2021YFC3001002), the National Natural Science Foundation of China (51879107), the Science and Technology Planning Project of Guangdong Province in China (2020A0505100009), the Water Resource Science and Technology Innovation Program of Guangdong Province (2020-28), and the Open Fund of State Key Laboratory of Subtropical Building Science (2021ZB23).

Appendix A. Supplementary data

Supplementary data to this article can be found online at https://doi.org/10.1016/j.jhydrol.2022.128113.

References

Alves, A., Gersonius, B., Kapelan, Z., Vojinovic, Z., Sanchez, A., 2019. Assessing the Co-Benefits of green-blue-grey infrastructure for sustainable urban flood risk management. J. Environ. Manage. 239, 244–254.

Bach, P.M., McCarthy, D.T., Urich, C., Sitzenfrei, R., Kleidorfer, M., Rauch, W., Deletic, A., 2013. A planning algorithm for quantifying decentralised water management opportunities in urban environments. Water Sci. Technol. 68, 1857–1865.

Bach, P.M., Deletic, A., Urich, C., McCarthy, D.T., 2018. Modelling characteristics of the urban form to support water systems planning. Environ. Modell. Softw. 104, 249–269.

Bonneau, J., Fletcher, T.D., Costelloe, J.F., Burns, M.J., 2017. Stormwater infiltration and the 'urban karst'–A review. J. Hydrol. 552, 141–150.

Chan, F.K.S., Griffiths, J.A., Higgitt, D., Xu, S., Zhu, F., Tang, Y.-T., Xu, Y., Thorne, C.R., 2018. "Sponge City" in China—a breakthrough of planning and flood risk management in the urban context. Land Use Pol. 76, 772–778.

Chang, Q., Kazama, S., Touge, Y., Aita, S., 2019. The effects of spatial discretization on performances and parameters of urban hydrological model. Water Sci. Technol. 80 (3), 517–528.

Chen, G., Chen, K., Yang, K., Guo, Q., 2021. Temporal and Spatial Distribution Characteristics of Precipitation over Guangzhou, China, IOP Conf. Ser.: Earth Environ. Sci. IOP Publishing, pp. 012024.

Chen, W., Huang, G., Zhang, H., Wang, W., 2018. Urban inundation response to rainstorm patterns with a coupled hydrodynamic model: A case study in Haidian Island. China. J. Hydrol. 564, 1022–1035.

Chui, T.F.M., Liu, X., Zhan, W., 2016. Assessing cost-effectiveness of specific LID practice designs in response to large storm events. J. Hydrol. 533, 353–364.

Damodaram, C., Zechman, E.M., 2013. Simulation-optimization approach to design low impact development for managing peak flow alterations in urbanizing watersheds. J. Water Resour. Plann. Manage. 139, 290–298.

Deb, K., 2014. Multi-objective optimization, Search methodologies. Springer, pp. 403-449.

Dietz, M.E., 2007. Low impact development practices: A review of current research and recommendations for future directions. Water, air, and soil pollution 186 (1), 351–363.

Duan, H.-F., Li, F., Yan, H., 2016. Multi-Objective Optimal Design of Detention Tanks in the Urban Stormwater Drainage System: LID Implementation and Analysis. Water Resour. Manage. 30 (13), 4635–4648.

Elliott, A., Trowsdale, S.A., 2007. A review of models for low impact urban stormwater drainage. Environ. Modell. Softw. 22 (3), 394–405.

Fletcher, T.D., Shuster, W., Hunt, W.F., Ashley, R., Butler, D., Arthur, S., Trowsdale, S., Barraud, S., Semadeni-Davies, A., Bertrand-Krajewski, J.-L., 2015. SUDS, LID, BMPs, WSUD and more–The evolution and application of terminology surrounding urban drainage. Urban Water J. 12 (7), 525–542.

Ghosh, I., Hellweger, F.L., 2012. Effects of spatial resolution in urban hydrologic simulations. J. Hydrol. Eng. 17 (1), 129–137.

Gironás, J., Roesner, L.A., Rossman, L.A., Davis, J., 2010. A new applications manual for the Storm Water Management Model(SWMM). Environ. Modell. Softw. 25 (6), 813–814.

Goldstein, A., Foti, R., Montalto, F., 2016. Effect of spatial resolution in modeling stormwater runoff for an urban block. J. Hydrol. Eng. 21 (11), 06016009.

Gunantara, N., 2018. A review of multi-objective optimization: Methods and its applications. Cogent Eng. 5 (1), 1502242. https://doi.org/10.1080/23311916.2018.1502242.

Huang, C.-L., Hsu, N.-S., Liu, H.-J., Huang, Y.-H., 2018. Optimization of low impact development layout designs for megacity flood mitigation. J. Hydrol. 564, 542–558.

Huang, M., Jin, S., 2019. A methodology for simple 2-D inundation analysis in urban area using SWMM and GIS. Natural Hazards 97, 15–43.

Huo, J., Liu, L., Zhang, Y., 2016. Comparative research of optimization algorithms for parameters calibration of watershed hydrological model. J. Comput. Methods Sci. Eng. 16 (3), 653–669.

Islam, A., Hassini, S., El-Dakhakhni, W., 2021. A systematic bibliometric review of optimization and resilience within low impact development stormwater management practices. J. Hydrol. 599, 126457.

Jacobson, C.R., 2011. Identification and quantification of the hydrological impacts of imperviousness in urban catchments: A review. J. Environ. Manage. 92 (6), 1438–1448.

Javadinejad, S., Eslamian, S., Ostad-Ali-Askari, K., 2021. The analysis of the most important climatic parameters affecting performance of crop variability in a changing climate. Int. J. Hydrol. Sci. Technol. 11, 1–25.

Javadinejad, S., Ostad-Ali-Askari, K., Jafary, F., 2019. Using simulation model to determine the regulation and to optimize the quantity of chlorine injection in water distribution networks. Model. Earth Syst. Environ. 5, 1015–1023.

Jia, H., Yao, H., Tang, Y., Shaw, L.Y., Field, R., Tafuri, A.N., 2015. LID-BMPs planning for urban runoff control and the case study in China. J. Environ. Manage. 149, 65–76.

Keifer, C.J., Chu, H.H., 1957. Synthetic storm pattern for drainage design. J. Hydraul. Divis., 83(4), 1332-1-1332-25.

Keshavarzzadeh, A.H., Ahmadi, P., 2019. Multi-objective techno-economic optimization of a solar based integrated energy system using various optimization methods. Energy Convers. Manage. 196, 196–210.

Kukkonen, S., Lampinen, J., 2005. GDE3: The third evolution step of generalized differential evolution, 2005 IEEE congress on evolutionary computation. IEEE 443–450.

Kuller, M., Bach, P.M., Ramirez-Lovering, D., Deletic, A., 2017. Framing water sensitive urban design as part of the urban form: A critical review of tools for best planning practice. Environ. Modell. Softw. 96, 265–282.

Li, S., Wang, Z., Lai, C., Lin, G., 2020. Quantitative assessment of the relative impacts of climate change and human activity on flood susceptibility based on a cloud model. J. Hydrol. 588, 125051.

Li, S., Wang, Z., Wu, X., Zeng, Z., Shen, P., Lai, C., 2022. A novel spatial optimization approach for the cost-effectiveness improvement of LID practices based on SWMM-FTC. J. Environ. Manage. 307, 114574.

Lai, F.-H., Dai, T., Zhen, J., Riverson, J., Alvi, K., Shoemaker, L., 2007. SUSTAIN-AN EPA BMP process and placement tool for urban watersheds. Proceedings of the Water Environment Federation 2007 (5), 946–968.

Lai, C., Chen, X., Wang, Z., Yu, H., Bai, X., 2020. Flood Risk Assessment and Regionalization from Past and Future Perspectives at Basin Scale. Risk Anal. 40 (7), 1399–1417.

Lee, J.-M., Hyun, K.-H., Choi, J.-S., 2013. Analysis of the impact of low impact development on runoff from a new district in Korea. Water Sci. Technol. 68 (6), 1315–1321.

Lee, J.G., Selvakumar, A., Alvi, K., Riverson, J., Zhen, J.X., Shoemaker, L., Lai, F.-H., 2012. A watershed-scale design optimization model for stormwater best management practices. Environ. Modell. Softw. 37, 6–18.

Li, F., Yan, X.-F., Duan, H.-F., 2019. Sustainable Design of Urban Stormwater Drainage Systems by Implementing Detention Tank and LID Measures for Flooding Risk Control and Water Quality Management. Water Resour. Manage. 33 (9), 3271–3288.

Liu, G., Chen, L., Shen, Z., Xiao, Y., Wei, G., 2019. A fast and robust simulation-optimization methodology for stormwater quality management. J. Hydrol. 576, 520–527.

Liu, Y., Ahiablame, L.M., Bralts, V.F., Engel, B.A., 2015. Enhancing a rainfall-runoff model to assess the impacts of BMPs and LID practices on storm runoff. J. Environ. Manage. 147, 12–23.

Liu, Y., Theller, L.O., Pijanowski, B.C., Engel, B.A., 2016. Optimal selection and placement of green infrastructure to reduce impacts of land use change and climate change on hydrology and water quality: An application to the Trail Creek Watershed, Indiana. Sci. Total Environ. 553, 149–163.

Mani, M., Bozorg-Haddad, O., Loáiciga, H.A., 2019. A new framework for the optimal management of urban runoff with low-impact development stormwater control measures considering service-performance reduction. J. Hydroinf. 21 (5), 727–744. https://doi.org/10.2166/hydro.2019.126.

Mao, X., Jia, H., Shaw, L.Y., 2017. Assessing the ecological benefits of aggregate LID-BMPs through modelling. Ecol. Modell. 353, 139–149.

Marlow, D.R., Moglia, M., Cook, S., Beale, D.J., 2013. Towards sustainable urban water management: A critical reassessment. Water Res. 47 (20), 7150–7161.

Marsalek, J., Watt, W., 1984. Design storms for urban drainage design. Can. J. Civ. Eng. 11 (3), 574–584.

Mei, C., Liu, J., Wang, H., Yang, Z., Ding, X., Shao, W., 2018. Integrated assessments of green infrastructure for flood mitigation to support robust decision-making for sponge city construction in an urbanized watershed. Sci. Total Environ. 639, 1394–1407.

Moriasi, D.N., Arnold, J.G., Van Liew, M.W., Bingner, R.L., Harmel, R.D., Veith, T.L., 2007. Model evaluation guidelines for systematic quantification of accuracy in watershed simulations. Trans. ASABE 50 (3), 885–900.

Nash, J.E., Sutcliffe, J.V., 1970. River flow forecasting through conceptual models part I—A discussion of principles. J. Hydrol. 10 (3), 282–290.

Oraei Zare, S., Saghafian, B., Shamsai, A., 2012. Multi-objective optimization for combined quality–quantity urban runoff control. Hydrol. Earth Syst. Sci. 16 (12), 4531–4542.

Ostad-Ali-Askari, K., Ghorbanizadeh Kharazi, H., Shayannejad, M., Zareian, M.J., 2020. Effect of climate change on precipitation patterns in an arid region using GCM models: case study of Isfahan-Borkhar Plain. Nat. Hazard. Rev. 21, 04020006.

Ostad-Ali-Askari, K., Shayannejad, M., Ghorbanizadeh-Kharazi, H., 2017. Artificial neural network for modeling nitrate pollution of groundwater in marginal area of Zayandeh-rood River, Isfahan. Iran. KSCE J. Civ. Eng. 21, 134–140.

Papalexiou, S.M., Montanari, A., 2019. Global and regional increase of precipitation extremes under global warming. Water Resour. Res. 55 (6), 4901–4914.

Pour, S.H., Abd Wahab, A.K., Shahid, S., Asaduzzaman, M., Dewan, A., 2020. Low impact development techniques to mitigate the impacts of climate-change-induced urban floods: Current trends, issues and challenges. Sustain. Cit. Soc. 62, 102373.

Qin, H.-P., Li, Z.-X., Fu, G., 2013. The effects of low impact development on urban flooding under different rainfall characteristics. J. Environ. Manage. 129, 577–585.
Quresh, K., Rahnamayan, S., He, Y., Liscano, R., 2019. Enhancing lqr controller using optimized real-time system by gde3 and nsga-ii algorithms and comparing with conventional method, 2019 IEEE Congress on Evolutionary Computation (CEC). IEEE 2074–2081.
Randall, M., Sun, F., Zhang, Y., Jensen, M.B., 2019. Evaluating Sponge City volume capture ratio at the catchment scale using SWMM. J. Environ. Manage. 246, 745–757.
Rosa, D.J., Clausen, J.C., Dietz, M.E., 2015. Calibration and verification of SWMM for low impact development. JAWRA J. Am. Water Resour. Associat. 51 (3), 746–757.
Rossman, L.A., 2010. Storm water management model user's manual, version 5.0. National Risk Management Research Laboratory, of Research and Development, US Environmental Protection Agency.
Rossman, L.A., Huber, W.C., 2015. Storm water management model reference manual volume I–Hydrology. U.S. EPA Office of Research and Development, Washington, DC, EPA/600/R-15/162A.
Shaneyfelt, K.M., Johnson, J.P., Hunt, W.F., 2021. Hydrologic Modeling of Distributed Stormwater Control Measure Retrofit and Examination of Impact of Subcatchment Discretization in PCSWMM. J. Sustainable Water Built Environ. 7 (3), 04021008.
Sun, N., Hall, M., Hong, B., Zhang, L., 2014. Impact of SWMM catchment discretization: case study in Syracuse. New York. J. Hydrol. Eng. 19 (1), 223–234.
Vargas, D.E., Lemonge, A.C., Barbosa, H.J., Bernardino, H.S., 2021. Solving multi-objective structural optimization problems using GDE3 and NSGA-II with reference points. Eng. Struct. 239, 112187.
Wu, X., Wang, Z., Guo, S., Liao, W., Zeng, Z., Chen, X., 2017. Scenario-based projections of future urban inundation within a coupled hydrodynamic model framework: a case study in Dongguan City. China. J. Hydrol. 547, 428–442.
Xu, T., Engel, B.A., Shi, X., Leng, L., Jia, H., Shaw, L.Y., Liu, Y., 2018. Marginal-cost-based greedy strategy (MCGS): Fast and reliable optimization of low impact development (LID) layout. Sci. Total Environ. 640, 570–580.
Xu, T., Jia, H., Wang, Z., Mao, X., Xu, C., 2017. SWMM-based methodology for block-scale LID-BMPs planning based on site-scale multi-objective optimization: a case study in Tianjin. Front. Env. Sci. Eng. 11 (4), 1. https://doi.org/10.1007/s11783-017-0934-6.
Yazdi, M.N., Ketabchy, M., Sample, D.J., Scott, D., Liao, H., 2019. An evaluation of HSPF and SWMM for simulating streamflow regimes in an urban watershed. Environ. Modell. Softw. 118, 211–225.
Yilmaz, A., Hossain, I., Perera, B., 2014. Effect of climate change and variability on extreme rainfall intensity–frequency–duration relationships: a case study of Melbourne. Hydrol. Earth Syst. Sci. 18 (10), 4065–4076.
Yin, D., Evans, B., Wang, Q., Chen, Z., Jia, H., Chen, A.S., Fu, G., Ahmad, S., Leng, L., 2020. Integrated 1D and 2D model for better assessing runoff quantity control of low impact development facilities on community scale. Sci. Total Environ. 720, 137630.
Zelinka, I., Snasael, V., Abraham, A., 2012. Handbook of optimization: from classical to modern approach. Springer Science & Business Media, p. 38.
Zeng, J., Huang, G., Luo, H., Mai, Y., Wu, H., 2019. First flush of non-point source pollution and hydrological effects of LID in a Guangzhou community. Sci. Rep. 9 (1), 1–10.
Zeng, J., Huang, G., Mai, Y., Chen, W., 2020. Optimizing the cost-effectiveness of low impact development (LID) practices using an analytical probabilistic approach. Urban Water J. 17 (2), 136–143. https://doi.org/10.1080/1573062X.2020.1748208.
Zeng, Z., Wang, Z., Lai, C., 2022. Simulation performance evaluation and uncertainty analysis on a coupled inundation model combining SWMM and WCA2D. Int. J. Disaster Risk Sci., Doi: 10.1007/s13753-022-00416-3.
Zhang, D.-L., 2020. Rapid urbanization and more extreme rainfall events. Sci. Bull. 65 (7), 516–518.
Zhang, G., Hmlett, J., Reed, P., Tang, Y., 2013. Multi-objective optimization of low impact development designs in an urbanizing watershed. Open J Optim 2, 95–108.
Zhang, K., Chui, T.F.M., 2018. A comprehensive review of spatial allocation of LID-BMP-GI practices: Strategies and optimization tools. Sci. Total Environ. 621, 915–929.
Zhang, M., Xu, M., Wang, Z., Lai, C., 2021. Assessment of the vulnerability of road networks to urban waterlogging based on a coupled hydrodynamic model. J. Hydrol. 127105.
Bisht, D.S., Chatterjee, C., Kalakoti, S., Upadhyay, P., Sahoo, M., Panda, A., 2016. Modeling urban floods and drainage using SWMM and MIKE URBAN: a case study. Natural Hazards 84, 749–776.